Dissolution and Crystallization Behavior of Poly(ethylene terephthalate)–Diluent Mixtures

L. M. VANE and F. RODRIGUEZ*

School of Chemical Engineering, Olin Hall, Cornell University, Ithaca, New York 14853

SYNOPSIS

The solution crystallization kinetics and crystal dissolution behavior of three grades of poly(ethylene terephthalate) in *N*-methyl-2-pyrrolidinone were studied using turbidimetric and calorimetric methods. The influence of concentration on the equilibrium dissolution temperature was described using Flory's melting point-composition relationship. The effect of the solvent alkyl group was also investigated. *N*-Methyl-2-pyrrolidinone was found to be a better solvent than *N*-ethyl-2-pyrrolidinone or *N*-cyclohexyl-2-pyrrolidinone for poly(ethylene terephthalate). From the calorimetric experiments, it was determined that two crystallization processes (primary and secondary crystallization) were responsible for the total crystallinity. The primary process dominated the early stages of the crystallization process and accounted for the majority of the final crystallinity for lower polymer concentrations. Based on coherent secondary nucleation theory, the effect of the crystallization temperature on the primary crystallization rate constant was quantified in terms of a temperature coefficient. This temperature coefficient was found to be relatively insensitive to PET concentration, PET structural impurities, and solvent alkyl group. © 1993 John Wiley & Sons, Inc.

INTRODUCTION

The solid-waste dilemma faced by many municipalities today as well as the economic value inherent to polymers has spurred research into the separation and reuse of postconsumer plastics. Common methods for separating mixed plastics include air classification, hydrocycloning, flotation–sedimentation, depolymerization–purification–repolymerization, and selective dissolution. Of these, only selective dissolution is capable of removing bound impurities from the plastic as well as differentiating plastics based on the chemical properties of the individual polymers without breaking down the polymer molecule. Therefore, selective dissolution processes should yield high-purity polymers that retain the economic value added by the initial polymerization reaction and can replace virgin resins in high-grade applications. Unfortunately, the higher purity achieved with a selective dissolution process comes at a higher price, resulting from the complexity of equipment and higher energy requirements as compared to density separation processes.

In an effort to lower the costs while maintaining the purity, an approach that combined low-cost, low-purity technologies with a multiple solvent selective dissolution process was proposed and applied, conceptually, to a 2 L bottle waste stream composed primarily of high-density polyethylene (HDPE) and poly(ethylene terephthalate) (PET).[1–4] Using a low-cost sink-float stage, the 2 L bottle waste would be separated into polyolefin and PET fractions, these fractions would then be sent to solvent-processing trains. Research efforts were concentrated on the selection and evaluation of solvents for the PET processing train. Based on the selection criteria of cost, solvent recovery, PET–solvent compatibility, HDPE–solvent incompatibility, and toxicity, the industrial solvent *N*-methyl-2-pyrrolidinone (NMP) was chosen. The dissolution behavior of 2 L bottle PET and HDPE in NMP has been presented previously.[1–4]

* To whom correspondence should be addressed.

Journal of Applied Polymer Science, Vol. 49, 765–776 (1993)
 CCC 0021-8995/93/050765-12

To better understand the interactions of PET and NMP, the dissolution behavior and crystallization kinetics of bottle-grade PET in NMP have been studied. The results of dilatometric solution crystallization experiments along with turbidimetric dissolution and crystallization experiments of one commercial grade of PET in NMP have been discussed elsewhere.[2]

The goal of this paper is to expand the understanding of the solution crystallization and dissolution behavior of PET and to further demonstrate the usefulness of turbidimetric crystallization and dissolution data. In this paper, it is shown that the dissolution behavior of PET crystals in NMP follows an established melting point–composition relationship. Also, calorimetric data on the solution crystallization of PET in NMP are introduced to confirm dilatometric observations regarding the occurrence of primary and secondary crystallization processes as well as to show the effect of crystallization conditions on the relative amounts of these two processes. In addition, the turbidimetric dissolution and solution crystallization behavior of two additional grades of PET in NMP are presented and compared to previously reported results in order to elucidate the impact of PET structural impurities. Similarly, the effect of changing the *N*-alkyl group of the solvent group *N*-alkyl-2-pyrrolidinone (NRP) on the solution crystallization and dissolution characteristics of PET has been investigated. Finally, the effect of the crystallization temperature on the primary crystallization process for all the PET/NRP samples is quantified in terms of a temperature coefficient derived using coherent secondary nucleation theory.

EXPERIMENTAL

Materials

Three grades of PET were used in the experiments: The majority of the samples were prepared with Goodyear Cleartuf 7207 resin [PET(7207)], which is commonly used in 2 L bottles with HDPE base cups. Other samples were prepared with Goodyear Cleartuf 8006 resin [PET(8006)], which can be used in 2 L bottles without base cups. PET(8006) is similar to PET(7207) except that a small amount of isophthalic acid is added to the terephthalic acid and ethylene glycol polymerization mixture, yielding a copolymeric PET that crystallizes more slowly. A third PET sample (HBPET) was melt and solid-state polymerized from bis(2-hydroxyethyl)terephthalate (BHET) (Polysciences) without catalysts or nucleating agents for comparison with the commercial PET samples.[3] The properties of these samples are presented in Table I. The three PET samples differ, structurally, with respect to the concentration of diethylene glycol (DEG) groups and isophthalate groups in the backbone of the polymer.

Procedures

Turbidimetry

The turbidimeter apparatus and sample preparation have been described in detail elsewhere.[2,3] Briefly, all samples analyzed with the turbidimeter were prepared from vacuum-dried PET and one of the following solvents: anhydrous *N*-methyl-2-pyrrolidinone (NMP) from Aldrich, molecular sieve-dried

Table I Properties of the PET Samples

Property	Type of PET		
	PET(7207)	PET(8006)	HBPET
Intrinsic viscosity in *o*-chlorophenol (dL/g) at 25°C	0.68	0.74	0.55
Number-average molecular weight (M_n)[a]	15,100	17,600	≈ 11,000
Catalyst content[5]	≈ 300 ppm	≈ 300 ppm	0
Mol % diethylene glycol (DEG)[b]	3.65	1.70	1.90
Mol % isophthalate[5]	0	≈ 2	0
Melting temp, T_m^0 (°C)[6]	260	—	265

[a] Based on gel permeation chromatographic analysis.
[b] Determined with NMR at 40°C in deuterated trifluoroacetic acid.

N-ethyl-2-pyrrolidinone (NEP), or molecular sieve-dried *N*-cyclohexyl-2-pyrrolidinone (CHP). The NEP and CHP were donated by GAF Chemicals. To avoid contamination by water, the solvents were transferred to the glass cells in a nitrogen-filled glove bag. The PET, solvent, and a Teflon-coated magnetic stirring bar were vacuum flame-sealed into glass cells (28 mm OD) with a final sample volume of about 35 mL.

The turbidimeter used to monitor the development of crystallinity and the dissolution of the polymer crystals was similar to that commonly used to determine cloud points and clearing points of noncrystalline polymer solutions.[7-12] For these experiments, the flame-sealed sample cells were immersed in a silicone oil bath (50 cs). The temperature of the bath was controlled using a proportional resistance temperature detector (RTD) controller (Omega Engineering CN2042) that was capable of maintaining the temperature to within ±0.1°C and was also able to increase the temperature at a constant rate. The cloudiness of the sample was determined by passing a He—Ne laser beam (Spectra-Physics 145-01 4 mW) through the sample. The intensity of the transmitted laser beam was converted to a voltage signal using a photodetector (United Detector Technologies PIN10DP) and current-to-voltage converter/amplifier.[3] The temperature of the bath was measured using an RTD probe. The resistance of the RTD probe was converted to a voltage signal (Omega Engineering TAC81-RTD converter) and amplified. Both the photosignal (V) and temperature voltages were recorded using a Data Translation DT2801 data acquisition board installed in an IBM personal computer. Data from the two signals were stored and analyzed with the aid of the Asystant+ software package (Macmillan Software Co.).

A flame-sealed sample was dissolved by immersing the cell in a second oil bath at an elevated temperature. Once the PET had dissolved, the cell was placed in the turbidimeter bath at the desired crystallization temperature (T_c) and acquisition of the photosignal data was initiated. As the crystallization proceeded, the photosignal became gradually attenuated until a final base line (V_f) was reached. A good measure of the time scale of the overall crystallization process is the time required for a 20% net reduction in the photosignal ($t_{0.2}^{ph}$). This occurs at the point where $(V_i - V) = 0.2(V_i - V_f)$. In this relationship, V_i is the initial base-line voltage. This parameter, $t_{0.2}^{ph}$, will be referred to as the "20% photosignal reduction time."

To determine the dissolution temperature (T_d) of the crystalline material formed in turbidimetric experiments, once the photosignal in the isothermal crystallization experiment had dropped approximately 90%, the cells were heated in the turbidimeter from the crystallization temperature until the solution cleared as a result of crystal dissolution. A heating rate of 1°C/min was used. During the heating process, the photosignal and bath temperature were recorded. The dissolution temperature was defined as the intersection of the final photosignal base line and the maximum slope line of the photosignal vs. the temperature dissolution curve. This type of dissolution measurement has been commonly used.[11,13,14] The dissolution temperature is generally a linear function of the crystallization temperature (T_c). The equilibrium dissolution temperature (T_d^0), the theoretical temperature at which perfect, infinitely thick crystals are in equilibrium with solvated polymer chains,[15] was estimated by extrapolating T_d vs. T_c data to the $T_d = T_c$ line. This extrapolation is commonly referred to as a Hoffman–Weeks plot.[13-18] Examples of this T_d^0 determination method have been presented previously for PET/NMP samples.[2,3] Theoretically, at this temperature, T_d^0, the solution is in crystallization/dissolution equilibrium and the crystallization of PET will take an infinite amount of time. It is the distance from T_d^0 ($\Delta T = T_d^0 - T_c$) that controls the rate of crystallization.

Dilatometry

A custom-made dilatometer with a sample volume of about 80 mL was used to measure the extent-of-crystallization over the entire crystallization process for three PET(7207)/NMP samples. The results of these experiments as well as details of the design and operation of the dilatometer have been provided elsewhere.[2,3]

Calorimetry

A Perkin-Elmer DSC-2C differential scanning calorimeter (DSC) equipped with an Intracooler II refrigeration unit, which allowed for cooling rates up to 320°C/min, was used to study the solution crystallization of PET in NMP. DSC samples of 3.0 and 9.0 wt % PET(7207) in anhydrous NMP (Aldrich) were prepared. All samples were sealed in aluminum volatile sample pans (Perkin-Elmer #0219-0062). A section of an aluminum DSC sample pan lid sealed in a volatile sample pan was used as the reference material. The PET/NMP samples were prepared

by vacuum flame-sealing the solvent and polymer in 10 mL Pyrex ampules. The polymer was dissolved by heating the ampules in an oven to 170°C for about 1 h. Once dissolved, the samples were cooled to room temperature to crystallize the polymer. The ampules were then opened in a nitrogen-filled glove bag, and about 13 mg of the PET/NMP suspensions were transferred to the DSC sample pans.

The DSC samples were studied using an endothermic method. In this method, a sample was heated to 170°C to dissolve the polymer, held for 4 min, and quenched to the crystallization temperature (T_c) at a rate of 160°C/min. After crystallizing at T_c for time, t_c, the sample was heated at a rate of 10°C/min while the energy and temperature signals from the instrument were recorded (endotherm). This procedure was repeated at the same T_c, for increasing crystallization times, until the resulting endotherm did not change in size or shape. The energy signal associated with a short crystallization time (less than 1 min) was used as the reference base line for the samples. DSC energy range settings of 0.1 and 0.2 mcal/s were used for 3.0 and 9.0 wt % samples, respectively.

RESULTS AND DISCUSSION

Solution Crystallization–Calorimetric Observations

Based on previous dilatometric experiments with PET/NMP samples containing 0.78, 1.7, and 3.3 wt % PET(7207), it appeared that the total crystallinity resulted from two processes: a primary process that accounted for the majority of the final crystallinity and dominated the early stages of the process, and a slower secondary process.[2,3] Under the assumption that two processes were occurring, the total extent-of-crystallization (X_T) was modeled as a weighted sum of the processes:

$$X_T = \omega_1 X_1 + (1 - \omega_1) X_2 \qquad (1)$$

where ω_1 is the fraction of the final crystallinity due to the primary process and X_i is the extent-of-crystallization of the ith process.

Furthermore, it was observed from the dilatometer experiments that the primary process was responsible for almost all of the crystallization in the early stages as well as the majority of the final crystallinity. This primary crystallization process was described using a standard Avrami equation:

$$X_1 = 1 - \exp(-kt^n) \qquad (2)$$

where X_1 is the extent-of-crystallization for the primary process; k, the Avrami rate constant; and n, the Avrami exponent. The rate constant, k, was determined using a novel derivative data analysis method.[2,3] The Avrami equation is commonly used to describe polymer crystallization from the melt [19–21] or from solution.[22,23] An Avrami exponent of $n = 4$ best described the data, indicating that primary crystallization resulted from homogeneous nucleation and three-dimensional growth.[19,22,24,25] Since the three-dimensional spherulitic growth of PET crystals is well documented[26–29] and spherulitic crystals from a PET/NMP solution were observed using an electron microscope,[3] an exponent of 4 was reasonable.

To verify the presence of multiple crystallization processes and to determine the effect of crystallization conditions on the relative amounts of these processes, the solution crystallization of PET in NMP was monitored with the calorimetric method described in the Experimental section. Two concentrations were studied with this method: 3.0 and 9.0 wt % PET(7207) in NMP. The change in the dissolution endotherm with crystallization time (t_c) for a 9.0 wt % PET(7207) in NMP sample crystallized at 95°C is illustrated in Figure 1. Initially, a crystal structure was formed that dissolved at about 133°C. Eventually, though, a second crystal structure ap-

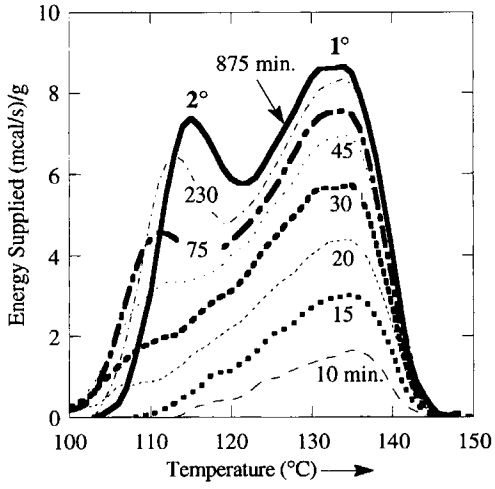

Figure 1 Effect of crystallization time (t_c) on the primary (1°) and secondary (2°) crystal dissolution peaks for 9.0 wt % PET(7207)/NMP crystallized at 95°C. Conditions: t_c = 10, 15, 20, 30, 45, 75, 230, and 875 min; heating rate = 10°C/min; range = 0.2 mcal/s. Signal normalized by sample mass.

peared that dissolved at about 114°C. The lower dissolution temperature of the secondary structure indicates that it was less stable than was the primary structure. It can also be seen in Figure 1 that the dissolution temperature of the secondary crystals increased with the crystallization time, whereas that of the primary crystals was invariant with respect to time. The increase in the dissolution temperature with time indicates that the secondary crystals underwent an annealing process that improved the stability of the crystal while the primary crystals were unaffected.[29]

The presence of two dissolution peaks suggests that two crystallization processes were present,[26,30,31] which confirms the conclusion from dilatometer experiments that primary and secondary crystallization processes caused the observed dilatometer height response.[2,3] In addition, it is apparent that the primary process dominates the overall crystallization during the initial stages of the crystallization as was also concluded from the dilatometric data. The primary peak (higher dissolution temperature) most likely represents spherulitic crystallization, while the secondary peak (lower dissolution temperature) may be associated with extraspherulitic crystallization.[26]

The effect of crystallization temperature on the dissolution endotherms is illustrated in Figure 2 for 9.0 wt % PET(7207) in NMP samples crystallized until completion at 90, 95, and 100°C. It is apparent

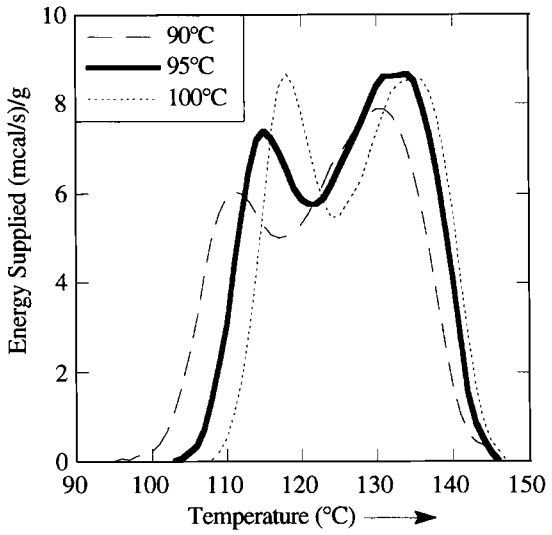

Figure 2 Effect of crystallization temperature on the dissolution endotherms of 9.0 wt % PET(7207)/NMP crystallized to completion. Signals normalized by mass of sample. Samples were estimated to be about 60% crystalline.

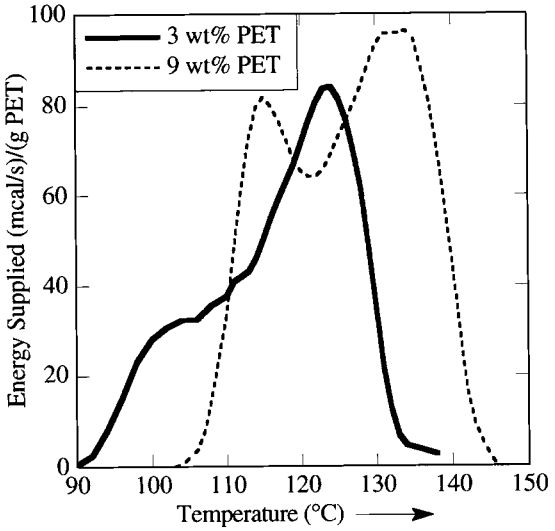

Figure 3 Effect of PET concentration on the endothermic dissolution peaks of PET(7207) in NMP crystallized to completion. Crystallization conditions: 725 min at 75°C for the 3.0 wt % sample and 875 min at 95°C for the 9.0 wt % sample. Heating rate: 10°C/min. Signals normalized by mass of PET in the sample.

that the dissolution temperatures of the primary and secondary crystal structures increased with increasing crystallization temperature. In addition, Figure 2 shows that the crystallization temperature affects the relative amount of secondary crystallization, as evidenced by the size of the secondary dissolution peak relative to that of the primary peak. Increasing T_c results in more secondary crystallization, probably a result of interactions between the growing crystals and the relative rates of the primary and secondary crystallization processes. Greater amounts of secondary crystallization at higher crystallization temperatures was also observed with dilatometer samples.[3]

The impingement and interaction of growing crystals can alter the character of the crystallization, promoting secondary crystallization. Reducing the polymer concentration should decrease these interactions and, therefore, the relative amount of secondary crystallization. From the dissolution endotherms for 3.0 and 9.0 wt % PET(7207) in NMP samples crystallized until completion at 75 and 95°C shown in Figure 3, it is evident that the size of the peak associated with the secondary crystals (relative to the size of the primary crystal endotherm) is much smaller for the 3.0 wt % sample. Therefore, in the PET/NMP samples, the relative amount of secondary crystallization was highly sensitive to concentration.

Solution Crystallization—Turbidimetric Results

As reported previously,[2,3] the development of crystallinity in dilatometer samples can be monitored with a turbidimetric method in which the time required for the onset of measurable cloudiness is used as a time scale for the primary crystallization process. It was observed that the dilatometrically determined Avrami rate constant, k, for the primary process could be related to the turbidimetrically determined time scale using the following power-law relationship:

$$k = \left(\frac{-\ln(0.9)}{\Phi^n}\right)\left(\frac{1}{t_{0.2}^{ph}}\right)^n \quad (3)$$

where $t_{0.2}^{ph}$ is the turbidimetric time scale and the parameter Φ is independent of temperature, but somewhat concentration-dependent.[2,3] As a result of this relationship, it is possible to use the more easily obtained turbidimetric data to study the effect of various crystallization conditions on the kinetics of the primary crystallization process.

The crystallization rate of a polymer is a function of several factors.[32,33] Prominent among these factors for solution crystallization are temperature, concentration, main-chain regularity, and solvent structure. The effect of crystallization temperature and PET(7207) concentration on the 20% photosignal reduction time ($t_{0.2}^{ph}$) and, therefore, the solution crystallization rate of PET(7207) in NMP, has already been reported.[2] $t_{0.2}^{ph}$ was found to be an exponential function of both the crystallization temperature and the polymer concentration.[2,3]

Effect of PET Structure

The regularity of the repeat units in a polymer chain impacts the ability of the polymer to crystallize by affecting its capacity to fit into a well-defined lattice. If the main chain is composed of a random mixture of units or contains a small amount of copolymer, it is more difficult for the molecule to fit into a repeating lattice structure. Chains with a greater degree of regularity will, therefore, crystallize faster and yield a higher final level of crystallinity.

To determine the effect of PET main-chain regularity on $t_{0.2}^{ph}$ and, therefore, the crystallization rate constant, flame-sealed samples of PET(8006) in NMP (0.89 wt %) and HBPET in NMP (0.88 wt %) were prepared and analyzed and compared with a 0.87 wt % PET(7207) in NMP sample. The values of $t_{0.2}^{ph}$ determined for these samples are displayed in Figure 4. These results indicate that for the same PET concentration and crystallization temperature, HBPET crystallizes most rapidly, followed by PET(7207) and PET(8006). This result is understandable since, from Table I, HBPET has the most regular structure (least amount of DEG) while the two Goodyear resins have higher levels of main-chain counits (DEG for the 7207 resin and DEG + isophthalate for the 8006 resin).

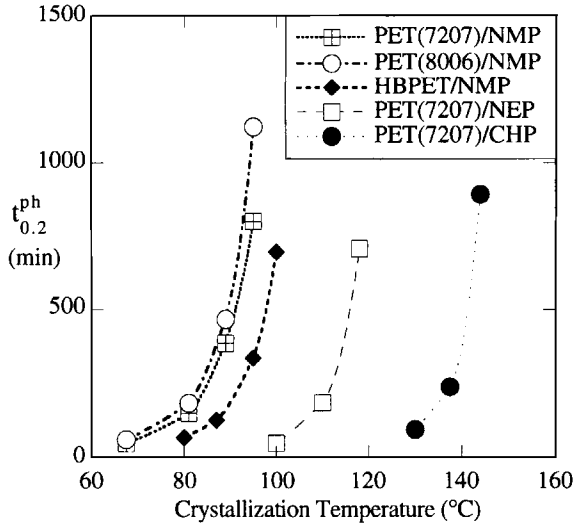

Figure 4 Variation of 20% photosignal reduction time ($t_{0.2}^{ph}$) with crystallization temperature (T_c) for flame-sealed samples of about 0.9 wt % PET(7207)/NMP, PET(8006)/NMP, HBPET/NMP, PET(7207)/NEP, and PET(7207)/CHP.

Effect of Solvent

Poly(ethylene terephthalate) is composed of two dissimilar moieties: an aliphatic ester group and an aromatic group. Because of this dissimilarity, PET exhibits a bimodal solubility parameter.[34–36] In other words, PET interacts with a solvent through two functional groups while many polymers interact through only one. As a result, the interactions between PET and a solvent are more complex than for a simple, single-unit polymer such as polyethylene. PET–solvent compatibility can be affected by changing the aromatic or aliphatic nature of the solvent, an important implication for the selection of the optimum solvent for a selective dissolution process. Therefore, the effect of the solvent alkyl group R (*N*-R-2-pyrrolidinone) on the dissolution and crystallization behavior of PET was investigated.

Flame-sealed samples of PET(7207) in NEP (R = ethyl group) and PET(7207) in CHP (R = cyclohexyl group) were prepared with concentrations of 0.90 and 0.97 wt %, respectively. In Figure 4, the

crystallization results for these two samples are presented together with those for the 0.87 wt % PET(7207) in NMP (R = methyl) sample [as well as the PET(8006)/NMP and HBPET/NMP samples]. These results indicate that increasing the size of the alkyl group of *N*-R-2-pyrrolidinone solvents increases the solution crystallization rate of PET (reduces compatibility). This observation is supported by Knox's work[34-36] in which it was found that the aromatic group of PET is capable of stronger interactions than those of the aliphatic ester group. Therefore, by increasing the aliphatic nature of the solvent (NMP < NEP < CHP), the PET–solvent interaction is worsened. Furthermore, a larger alkyl group introduces some steric hindrance, reducing the polymer–solvent compatibility.

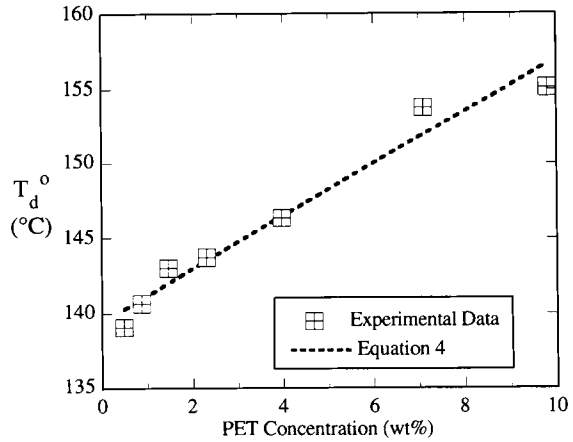

Figure 5 Influence of PET concentration on the equilibrium dissolution temperature (T_d^0) for flame-sealed samples of PET(7207) in NMP.

Dissolution Behavior

To understand the solution crystallization kinetics of a polymer, the dissolution characteristics of the polymer/solvent pair must be determined. The importance of the dissolution behavior lies in the driving force for the crystallization, which is the degree to which a polymer solution is cooled below the equilibrium dissolution temperature. As was the case for the crystallization rate, many factors affect the dissolution temperature of a polymer including concentration, crystallization temperature, main-chain regularity, and solvent. Some experimental data on the effect of polymer concentration and crystallization temperature on the dissolution temperature of PET(7207) in NMP have been reported previously[2]; however, the effect of PET concentration on the equilibrium dissolution temperature, T_d^0, was not thoroughly investigated.

Effect of PET Concentration

The dissolution behavior of seven flame-sealed PET(7207)/NMP samples was analyzed according to the procedure described in the Experimental section. The T_d^0 values determined in this manner are plotted in Figure 5 as a function of PET(7207) concentration. It is well documented that the melting point and glass transition temperature of a polymer are depressed by the addition of a diluent.[20,32] The extent of the depression depends on the structure of the solvent as well as the polymer–solvent compatibility. This effect has been extensively studied both theoretically and experimentally.[37-45] The theoretical development is based on the Flory–Huggins theory for the free energy of mixing of two species in a polymer melt.[46] Flory extended this theory to describe the melting point–composition relationship for mixtures of semicrystalline polymers and diluents.[40] This work is summarized by the following classic relationship:

$$\left(\frac{1}{T_d^0} - \frac{1}{T_m^0}\right) = \left(\frac{R}{\Delta H_u}\right)\left(\frac{V_u}{V_1}\right)[\nu_1 - \chi_1(\nu_1)^2] \quad (4)$$

where T_d^0 is the equilibrium dissolution (melting) temperature for a polymer/solvent mixture with a solvent volume fraction ν_1. T_m^0 is the melting temperature of the pure polymer; V_1 and V_u, the molar volumes of the solvent and polymer repeat unit, respectively; ΔH_u, the heat of fusion of the pure polymer per mole of repeat units; R, the gas constant; and χ_1, the Flory–Huggins thermodynamic interaction parameter.

Equation (4) was used to fit the PET(7207)/NMP dissolution data. Literature values were used for all of the parameters except χ_1: $(V_u/V_1) = 1.35$; $T_m^0 = 260°C$ (533 K); $\Delta H_u = 6430$ cal/mol.[6,38,47-49] The polymer–solvent interaction parameter, χ_1, is often dependent upon the polymer concentration and can be represented as a polynomial expansion in terms of the polymer volume fraction (ν_2)[50]:

$$\chi_1 = \sum_{i=0}^{\infty} a_i(\nu_2)^i \quad (5)$$

where a_i are constants. For this work, only the first two terms in the expansion were retained; therefore, eq. (5) reduced to (in terms of the solvent volume fraction)

$$\chi_1 = (a_1 + a_2) - a_2\nu_1 \quad (6)$$

The best least-squares fit (R^2 = 0.97) of the PET(7207)/NMP dissolution data to eq. (4) was obtained with $\chi_1 = 1.7 - 2.0\nu_1$. This fitted equation is plotted in Figure 5 along with the experimental data. The interaction parameter ranged from −0.31 for 0.49 wt % PET to −0.17 for the 9.8 wt % PET sample. Positive values of χ_1 are more common than are negative values, but $\chi_1 < 0$ has been observed for several polymer–solvent systems including PET–dibutyl phthalate and poly(decamethylene terephthalate)–benzophenone.[20,39] It is evident from Figure 5 that the theoretical relationship [eq. (4)] represents the data quite well.

Effect of PET Structure

It was shown in a previous section that at a given crystallization temperature, HBPET crystallizes most rapidly, followed by PET(7207) and PET(8006). This trend may have resulted from differences in T_d^0 that would alter the crystallization driving force, $\Delta T = (T_d^0 - T_c)$. The dissolution and melting behavior of polymer crystals is affected by the same factors that control the crystallization behavior. In general, as the perfection of the crystal lattice increases, so too does the melting/dissolution temperature. Therefore, for a given polymer, if the regularity of repeat units is increased, then the melting/dissolution temperature will also increase. As a result, materials that contain small amounts of main-chain impurities will exhibit higher melting/dissolution temperatures than those with higher impurity levels. For example, diethylene glycol (DEG) groups in PET may occupy the positions of some ethylene glycol (EG) groups. It has been found that the T_m of PET is reduced 3°C for each mol % DEG in the polymer main chain.[6]

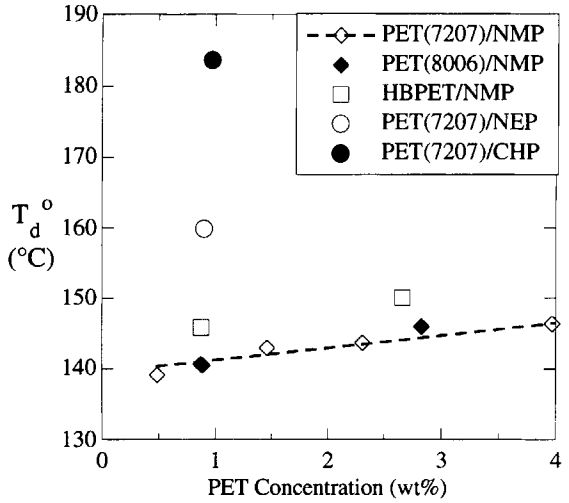

Figure 6 Variation of the equilibrium dissolution temperature (T_d^0) with concentration for all flame-sealed samples with PET concentrations in the range of 0–4 wt %.

To further investigate this trend, the dissolution behavior of two HBPET/NMP flame-sealed samples and two PET(8006)/NMP samples was determined. The variation of the equilibrium dissolution temperature with PET concentration is presented in Figure 6 for all flame-sealed samples in the concentration range of 0–4 wt %. It is apparent that T_d^0 for PET(8006) is about the same as that of PET(7207). On the other hand, T_d^0 for HBPET is almost 6°C higher than for PET(7207). This observed trend in T_d^0 values suggests that the driving force for crystallization is less for PET(7207) and PET(8006) than for HBPET, which explains why the 20% photosignal reduction time is much less for the HBPET/NMP system.

Effect of Solvent

The dissolution behavior of the 0.90 wt % PET(7207)/NEP and 0.97 wt % PET(7207)/CHP flame-sealed samples was studied. Based on the effect of the *N*-R-2-pyrrolidinone alkyl group (R) on $t_{0.2}^{ph}$, it was concluded that, of the solvents studied, NMP (R = methyl) was the best solvent for PET, followed by NEP (R = ethyl) and CHP (R = cyclohexyl). This trend in PET–solvent compatibility is confirmed by the dissolution results presented in Figure 6. For samples with about 0.9 wt % PET(7207), T_d^0 = 141°C for NMP, 160°C for NEP, and 183°C for CHP. These results provide confirmation that as the size of the alkyl group on the solvent is increased compatibility with PET is greatly reduced.

Temperature Coefficient of the Solution Crystallization Process

In the preceding sections, the effect of several factors on the solution crystallization rate of PET have been discussed. Of these factors, the crystallization temperature has the most dramatic effect. For this reason, an attempt was made to relate the crystallization rate to the crystallization temperature (T_c) using crystallization theory and observed relationships.

The temperature dependence of the crystallization process, as observed in Figure 7 for a dilatometer sample, results from the strong effect of temperature on the primary crystallization rate constant, k. This dependence can be described by the following relationship[23,28]:

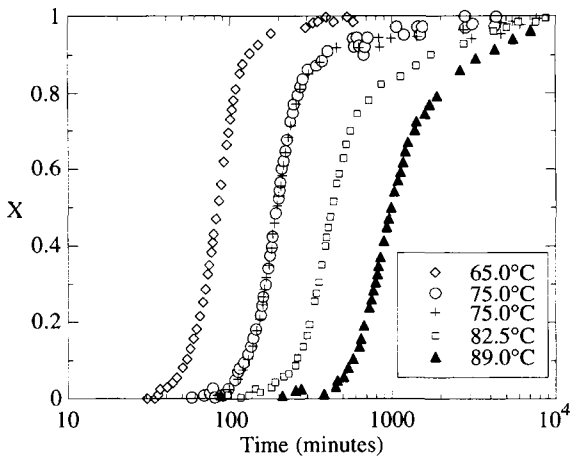

Figure 7 Plot of extent-of-crystallization (X) as a function of time and crystallization temperature for 0.78 wt % PET(7207) in NMP dilatometer sample.

$$k = k_0 \exp\left(\frac{p[-E_D - \Delta F^*]}{k_b T_c}\right) \tag{7}$$

where k_0 is a constant with respect to temperature but not concentration; p, a constant that describes the growth dimensionality; and k_b, the Boltzmann constant. E_D is the activation energy for transport that, for polymer solutions, is assumed to be negligible. ΔF^* is the free energy for the formation of a critical-sized secondary nucleus. For coherent secondary nucleation,[3,21,51,52]

$$\Delta F^* = \frac{4 b_0 \sigma \sigma_e T_d^0}{\Delta h_f \Delta T} \tag{8}$$

where ΔT is the crystallization driving force ($T_d^0 - T_c$); b_0, the monomolecular thickness of the nucleus; Δh_f, the heat of fusion per unit volume; and σ and σ_e, the lateral and end surface free energies of the crystal (units of erg/cm^2), respectively.

Combining eqs. (7) and (8) yields

$$\frac{-\log(k)}{n} = \frac{-\log(k_0)}{n} + \Theta\left(\frac{T_d^0}{T_c \Delta T}\right) \tag{9}$$

where the temperature coefficient, Θ, is a lumped constant assumed to be independent of temperature:

$$\Theta = \frac{4 b_0 \sigma \sigma_e (p/n)}{2.3 k_b \Delta h_f} \tag{10}$$

According to eq. (9), the logarithm of the rate constant varies linearly with $T_d^0/(T_c \Delta T)$. This is referred to as the "ΔT^{-1} rate law." The values of $-\log(k)/n$ for the three dilatometer samples[2,3] are plotted in Figure 8 as a function of $T_d^0/(T_c \Delta T)$. As suggested by eq. (9), a linear relationship results. The average slope of the lines (Θ) in Figure 8 is 154 $\pm$ 13 K. Using eq. 10, the product of the surface free energies ($\sigma\sigma_e$) for the PET crystals was estimated to be about 480 erg^2/cm^4 based on the average slope of the lines, $\Delta h_f = 2.0 \times 10^9$ erg/cm^3, $b_0 = 0.5$ nm, and $(p/n) = 1$. This value of $\sigma\sigma_e$ is the same order of magnitude as for other homopolymers such as poly(chlorotrifluoroethylene) (200 erg^2/cm^4), isotactic polystyrene (270 erg^2/cm^4), and poly(vinylidene fluoride) (370 erg^2/cm^4).[21,51,52]

The turbidimetric crystallization time can be related to the temperature parameters by combining eq. (3) with eq. (9) to yield

$$\log(t_{0.2}^{ph}) = B + \Theta\left(\frac{T_d^0}{T_c \Delta T}\right) \tag{11}$$

where Θ is the same as in eq. (9) and B is a lumped parameter that is independent of temperature but is sensitive to concentration. According to eq. (11), a plot of $\log(t_{0.2}^{ph})$ vs. $T_d^0/(T_c \Delta T)$ will be linear, with a slope of Θ. From Figure 9, it is apparent that eq. (11) is valid, since a linear relationship is observed for $t_{0.2}^{ph}$ data from the dilatometer samples. In addition, the slopes of the lines in Figure 9 are within about 1% of the corresponding lines in Figure 8, indicating that Θ is the same for both turbidimeter

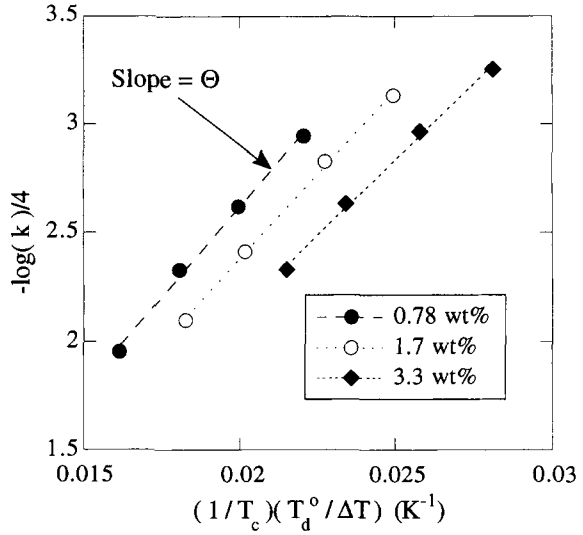

Figure 8 Plot of Avrami rate constant, k, as a function of $T_d^0/(T_c \Delta T)$ according to eq. (9) for the three PET(7207)/NMP dilatometer samples. The slopes of the lines for the 0.78, 1.7, and 3.3 wt % PET samples are 166, 155, and 140 K, respectively.

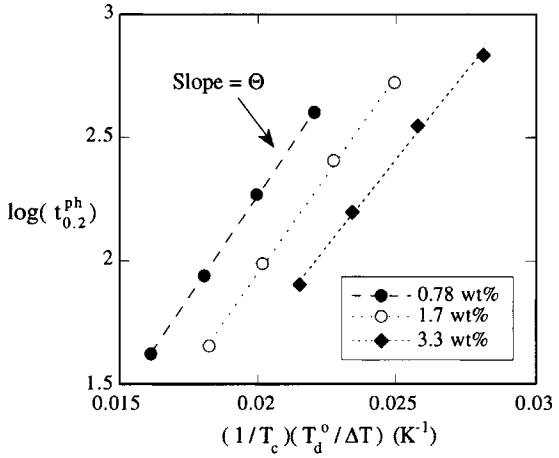

Figure 9 Plot of the 20% photosignal reduction time ($t_{0.2}^{ph}$) as a function of $T_d^0/(T_c\Delta T)$ according to eq. (11) for the three PET(7207)/NMP dilatometer samples. The slopes of the lines for the 0.78, 1.7, and 3.3 wt % PET samples are 166, 159, and 141 K, respectively.

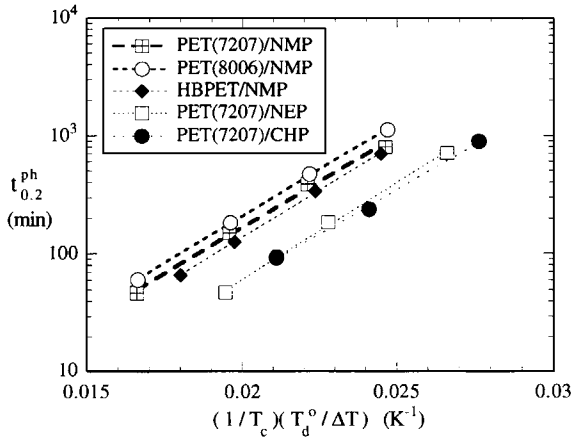

Figure 11 Plot of the 20% photosignal reduction time ($t_{0.2}^{ph}$) as a function of $T_d^0/(T_c\Delta T)$ according to eq. (11) for flame-sealed samples of about 0.9 wt % PET(7207)/NMP, PET(8006)/NMP, HBPET/NMP, PET(7207)/NEP, and PET(7207)/CHP.

data ($t_{0.2}^{ph}$) and dilatometer data (k). Therefore, the effect of crystallization conditions on the temperature coefficient (Θ) can be determined using more easily obtained turbidimetric data in place of rigorous dilatometric data.

Effect of Concentration, PET Structure, and Solvent on Temperature Coefficient

The effect of PET concentration on Θ for the dilatometer samples and the turbidimeter flame-sealed PET(7207) samples is illustrated in Figure 10. It appears that Θ decreases linearly with the logarithm of the PET concentration, most likely because of changes in the surface free energies (σ or σ_e) or because the model used to develop eq. (9) does not exactly describe the crystallization process.

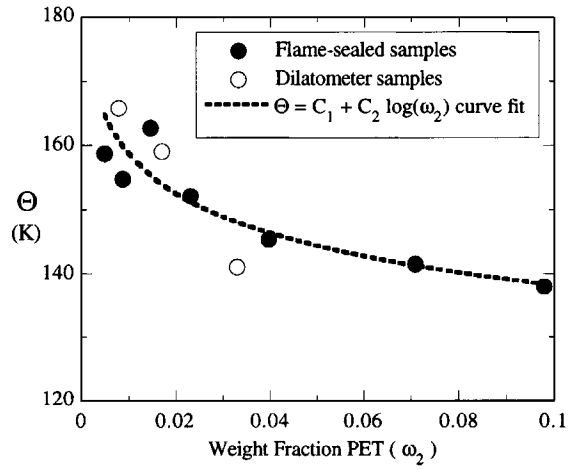

Figure 10 Variation of the temperature coefficient (Θ) with PET concentration for all PET(7207)/NMP samples.

In a previous section, it was observed that the solution crystallization rate of PET was significantly affected by the counit content (diethylene glycol and isophthalate) of the polymer backbone as well as by the solvent type. The $t_{0.2}^{ph}$ data for PET(8006)/NMP and HBPET/NMP flame-sealed samples are plotted vs. $T_d^0/(T_c\Delta T)$ in Figure 11 along with the data for the 0.87 wt % PET(7207)/NMP sample. Since the lines have similar slopes, it is clear that the temperature coefficient is relatively unaffected by changes in the counit content. On the other hand, the intercept is affected by the PET structure as evidenced by the vertical offset of the lines.

Similarly, the temperature coefficient was not found to be a function of the solvent alkyl group as evidenced by the similar slopes of the $t_{0.2}^{ph}$ vs. $T_d^0/(T_c\Delta T)$ data in Figure 11 for flame-sealed samples of PET(7207) in *N*-methyl-2-pyrrolidinone (NMP), *N*-ethyl-2-pyrrolidinone (NEP), and *N*-cyclohexyl-2-pyrrolidinone (CHP). This indicates that Θ and, therefore, the surface free energies, are independent of the crystallization medium. The same observation (Θ independent of solvent) was made by Devoy et al.[22] for the solution crystallization of polyethylene in decalin, *p*-xylene, and *n*-hexadecane.

CONCLUSIONS

The experimental techniques of dilatometry, turbidimetry, and calorimetry were applied to study the

solution crystallization of PET. Dilatometry was used to monitor the extent-of-crystallization directly. Two crystallization processes were found to be responsible for the total crystallinity: a primary process that accounted for the majority of the final crystallinity and dominated the first 60% of the process, and a slower secondary process. The Avrami rate constant, k, was found to be sensitive to the crystallization temperature and PET concentration.

Calorimetric experiments carried out on PET/NMP samples confirmed dilatometric observations that two crystallization processes were responsible for the total crystallinity and that the primary process dominated the early stages of the crystallization. It was also observed that the amount of secondary crystallization relative to the amount of primary crystallization was reduced by increasing the crystallization temperature or by lowering the PET concentration.

Turbidimetric experiments were found to have several advantages over dilatometric experiments: They do not require strict temperature control, they can be monitored with computer-based data acquisition systems, and the final state is reached at significantly shorter times, reducing the time required to analyze a sample. Using turbidimetry, the solution crystallization rate of PET was found to be sensitive to polymer concentration, crystallization temperature, polymer structure, and solvent. The dissolution temperature was also determined to be a function of these variables.

Based on secondary nucleation theory, a relationship between the crystallization temperature and the Avrami rate constant was developed. The relationship was extended to apply to turbidimetric data. The temperature coefficient in the relationship (Θ) was found to be a weak function of PET concentration, but virtually independent of both PET structure and solvent.

From the experimental results presented in this work, it is apparent that the solution crystallization behavior of poly(ethylene terephthalate) is a complex function of PET structure, PET concentration, temperature, and the solvent used. This complexity, especially with regard to PET structure, has serious implications for a postconsumer 2 L bottle selective dissolution process since the feed stream will be composed of a mixture of commercial grades of PET. Fortunately, the turbidimetric method developed for this work could be used to pretest the crystallization characteristics of the mixed PET feed and determine the optimum process conditions. In addition, turbidimeters could serve as on-line analysis instruments to detect the onset of crystallization in order to avoid clogging heat-exchanger tubes and solution purification filters. This information would also be useful if temperature quenching were used to recover the polymer from solution.

The authors wish to thank the Plastics Institute of America for research fellowships, the National Science Foundation and DuPont for stipend support, and the Goodyear Tire & Rubber Co. for PET samples.

REFERENCES

1. L. M. Vane and F. Rodriguez, presented at the *Soc. Plas. Eng. Reg. Tech. Conf.: Recycling of Plastic Materials to Meet Government and Industry Requirements,* November 29–30, 1990.
2. L. M. Vane and F. Rodriguez, in *Emerging Technologies in Plastics Recycling,* ACS Symposium Series No. 513, American Chemical Society, New York, 1992.
3. L. M. Vane, PhD Thesis, Cornell University, 1992.
4. F. Rodriguez, L. M. Vane, J. J. Schlueter, and P. Clark, in *Environmental Remediation,* ACS Symposium Series No. 509, American Chemical Society, New York, 1992.
5. A. Sawaya, Private communication.
6. J. Brandrup and E. H. Immergut, Eds., *Polymer Handbook,* 3rd ed., Wiley-Interscience: New York, 1989.
7. Z. Tong, Y. Einaga, H. Miyashita, and H. Fujita, *Macromolecules,* **20,** 1888 (1987).
8. Z. Tong, Y. Einaga, T. Kitagawa, and H. Fujita, *Macromolecules,* **22,** 450 (1989).
9. M. Tsuyumoto, Y. Einaga, and H. Fujita, *Polym. J.,* **16,** 229 (1984).
10. S. G. Stafford, A. C. Ploplis, and D. T. Jacobs, *Macromolecules,* **23,** 470 (1990).
11. M. Minagawa, K. Miyano, T. Morita, and F. Yoshii, *Macromolecules,* **22,** 2054 (1989).
12. A. R. Shultz and P. J. Flory, *J. Am. Chem. Soc.,* **74,** 4760 (1952).
13. J. F. Jackson and L. Mandelkern, *Macromolecules,* **1,** 546 (1968).
14. P. J. Lemstra and G. Challa, *J. Polym. Sci. Polym. Phys. Ed.,* **13,** 1809 (1975).
15. H. M. Schleinitz, *Anal. Calorim.,* **1,** 23 (1968).
16. J. D. Hoffman and J. J. Weeks, *J. Res. Nat. Bur, Stand.,* **66A,** 13 (1962).
17. P. C. Vilanova, S. M. Ribas, and G. M. Guzman, *Polymer,* **26,** 423 (1985).
18. W. H. Jo, I. H. Kwon, and C. Seoul, *Polym. Eng. Sci.,* **29,** 1569 (1989).
19. A. Sharples, *Introduction to Polymer Crystallization,* Edward Arnold, London, 1966.
20. L. Mandelkern, *Crystallization of Polymers,* McGraw-Hill, New York, 1964.
21. R. J. Ciora, Jr. and J. H. Magill, *Macromolecules,* **23,** 2350 (1990).
22. C. Devoy, L. Mandelkern, and L. Bourland, *J. Polym. Sci. Part A-2,* **8,** 869 (1970).

23. L. Mandelkern, *Polymer,* **5,** 637 (1964).
24. J. G. Fatou, C. Marco, and L. Mandelkern, *Polymer,* **31,** 890 (1989).
25. G. M. Stack, L. Mandelkern, C. Krohnke, and G. Wegner, *Macromolecules,* **22,** 4351 (1989).
26. S. A. Jabarin, *Polym. Eng. Sci.,* **29,** 1259 (1989).
27. S. A. Jabarin, *Polym. Eng. Sci.,* **24,** 376 (1984).
28. C. C. Lin, *Polym. Eng. Sci.,* **23,** 113 (1983).
29. L. J. Fina, and J. L. Koenig, *Macromolecules,* **17,** 2572 (1984).
30. M. Girolamo, A. Keller, K. Miyasaka, and N. Overbergh, *J. Polym. Sci. Polym. Phys. Ed.,* **14,** 39 (1976).
31. C. Zhou and S. B. Clough, *Polym. Eng. Sci.,* **28,** 65 (1988).
32. F. Rodriguez, *Principles of Polymer Systems,* 3rd ed., Hemisphere, New York, 1989.
33. J. M. Margolis, Ed., *Engineering Thermoplastics: Properties and Applications,* Marcel Dekker, New York, 1985.
34. B. H. Knox, *J. Appl. Polym. Sci.,* **21,** 225 (1977).
35. B. H. Knox, *J. Appl. Polym. Sci.,* **21,** 249 (1977).
36. B. H. Knox, *J. Appl. Polym. Sci.,* **21,** 267 (1977).
37. A. J. Pennings, *J. Polym. Sci. Part C,* **16,** 1799 (1967).
38. P. E. Slade and T. A. Orofino, *Anal. Calorim.,* **1,** 63 (1968).
39. L. Rebenfeld, P. J. Makarewicz, H-D. Weigmann, and G. L. Wilkes, *J. Macromol. Sci.-Rev. Macromol. Chem.,* **C15,** 279 (1976).
40. P. J. Flory, *J. Chem. Phys.,* **17,** 223 (1949).
41. W. M. Leung, R. St. J. Manley, and A. R. Panaras, *Macromolecules,* **18,** 746 (1985).
42. A. Prasad and L. Mandelkern, *Macromolecules,* **22,** 914 (1989).
43. A. Prasad and L. Mandelkern, *Polym. Prepr.,* **28,** 371 (1987).
44. J. A. Currie, E. M. Petruska, and R. W. Tung, *Anal. Calorim.,* **3,** 569 (1974).
45. A. Takahashi, T. Nakamura, and I. Kagawa, *Polym. J.,* **3,** 207 (1972).
46. P. J. Flory, *Principles of Polymer Chemistry,* Cornell University Press, Ithaca, NY, 1953.
47. P. Kneisl and J. W. Zondlo, *J. Chem. Eng. Data,* **32,** 11 (1987).
48. *M-Pyrol® N-Methyl-2-Pyrrolidone Handbook,* GAF Corp., New York, 1972.
49. A. Mehta, U. Gaur, and B. Wunderlich, *J. Polym. Sci. Polym. Phys. Ed.,* **16,** 289 (1978).
50. M. Kurata, *Thermodynamics of Polymer Solutions,* Harwood, New York, 1982.
51. Y. S. Yadav, P. C. Jain, and V. S. Nanda, *Thermo. Acta,* **80,** 231 (1984).
52. J. D. Hoffman and J. J. Weeks, *J. Chem. Phys.,* **37,** 1723 (1962).

Received August 17, 1992
Accepted October 28, 1992